Energy dissipation via the internal fracture of the silica particle network in inorganic/organic double network ion gels

Yasui, Tomoki
Fujinami, So
Hoshino, Taiki
Kamio, Eiji
Matsuyama, Hideto

ARTICLE

Energy Dissipation via the Internal Fracture of the Silica Particle Network in Inorganic/Organic Double Network Ion Gels

Received 00th January 20xx,
Accepted 00th January 20xx

DOI: 10.1039/x0xx00000x

Tomoki Yasui,[a] So Fujinami,[b] Taiki Hoshino,[b] Eiji Kamio,*[a] and Hideto Matsuyama*[a]

Inorganic/organic double network (DN) ion gels, which are composed of an inorganic silica particle network, an organic poly(*N,N*-dimethylacrylamide) (PDMAAm) network, and a large amount of ionic liquid, showed excellent mechanical strength over 25 MPa compression fracture stress at an 80 wt% ionic liquid content. The excellent mechanical strength of these inorganic/organic DN ion gels was attributed to the energy dissipation of the inorganic/organic DN structure. It has been considered that the energy dissipation in inorganic/organic DN ion gels is caused by the internal fracture of the silica particle network, which is preferentially fractured by deformation. However, no studies to investigate the internal fracture of the silica particle network in inorganic/organic DN ion gels have been conducted by direct approaches. In this study, the internal fracture of the silica particle network in the inorganic/organic DN ion gel was directly evaluated using a small angle X-ray scattering (SAXS). The synchrotron SAXS measurements conducted under a uniaxial loading–unloading process demonstrated that the aggregation size of the silica particle network irreversibly decreased with uniaxial stretch. Based on these results, it was clarified that the energy dissipation of the inorganic/organic DN ion gels was attributed to the internal fracture of the silica particle network.

Introduction

Ion gels are gels containing ionic liquids (ILs) that show quasi-solid properties in addition to IL-based properties such as nonvolatility, nonflammability, high ionic conductivity, high CO_2 solubility, and high thermal, chemical, and electrochemical stabilities. It is expected that ion gels will be applied in electrochemical devices, actuators, and gas separation membranes.[1–8] However, the practical application of ion gels is limited because of their low mechanical strength. Thus, the development of tough ion gels has attracted increasing interest.

Several kinds of tough ion gels have been prepared with several different concepts, such as tetra-PEG network-based ion gels[9], triblock copolymer-based ion gels[10], and organic/organic double network (DN)-based ion gels,[6,11–14] which are composed of interpenetrating polymer networks. These tough ion gels showed not only excellent mechanical strength, but also almost pure IL properties as the IL content was over 80 wt%. Recently, we fabricated DN-based tough ion gels using inorganic/organic composite DN.[15,16] The inorganic/organic DN was composed of a silica particle-based inorganic network and poly(*N*,*N*-dimethylacrylamide) (PDMAAm)-based organic network. The inorganic/organic DN ion gels showed excellent mechanical strength over 25 MPa compression fracture stress in spite of their 80 wt% IL content. We believe the inorganic/organic DN ion gel has two advantageous points compared with the organic/organic DN ion gels. One is the one-pot network formation. In general, the extensively studied organic/organic DN ion gels are prepared via successive two network formation process[14] or solvent exchange process[6,11–13]. Because both processes need swelling process, the preparation procedures are more complicate than the one-pot network formation. In addition, it is difficult to control the shape of the organic/organic DN ion gels because the shape of gels is changed via the swelling process. On the other hand, the inorganic/organic DN ion gels can be prepared via simple one-pot process. Owing to the one-pot network formation, the shapes of inorganic/organic DN ion gel can be easily controlled.[15] The other advantage is self-healing property of sacrificial bonds that is preferentially fractured by deformation. The organic/organic DN ion gels usually have chemically cross-linked polymeric sacrificial network, which cannot be recovered after destruction. On the other hand, the sacrificial bonds of the inorganic/organic DN ion gels are silica particle network. The silica particles were connected via the inter-particle interactions such as van der Waals attraction force and hydrogen bonding. Therefore, the fractured silica particle network can be recovered by annealing.[15]

In DN systems, including inorganic/organic DN and organic/organic DN systems, mechanical hysteresis has been observed on the stress–strain curve.[15–22] Thus, it has been demonstrated that the excellent mechanical strength of the

[a] *Research Center for Membrane and Film Technology, Department of Chemical Science and Engineering, Kobe University, 1-1 Rokkodai-cho, Nada-ku, Kobe, Hyogo 657-8501, Japan.*
[b] *RIKEN SPring-8 Center, 1-1-1 Kouto, Sayo-cho, Sayo-gun, Hyogo 679-5148, Japan*
E-mail: e-kamio@people.kobe-u.ac.jp; matuyama@kobe-u.ac.jp

Electronic Supplementary Information (ESI) available: Chemical structures of $[C_4mim][Tf_2N]$ and PDMAAm, high magnification TEM image of the silica particle network in the inorganic/organic DN ion gel, original SAXS profile of the inorganic/organic DN ion gel, horizontal SAXS profile of the inorganic/organic DN ion gel and PDMAAm SN ion gel without background analysis, and cyclic loading–unloading curves of PDMAAm SN ion gel. See DOI: 10.1039/x0xx00000x

inorganic/organic DN ion gels are due to the energy dissipation mechanism. A variety of studies have concluded that the energy dissipation in inorganic/organic DN and organic/organic DN systems is caused by the internal fracture of a sacrificial network.[15,17] However, no reports discuss the internal network fracture based on direct approaches, such as electron microscopy and X-ray scattering. In rubber system which composed of filler particle and polymer matrix, structural change of particle aggregation in rubber during deformation has been widely investigated in previous papers. However, these studies, including the report by Hashimoto et al.[23], mainly focused on the anisotropy of particle aggregation in deformed rubber. On the other hand, our study discusses the fracture phenomenon of particle aggregation network. In other words, here we discuss about the internal distraction of silica particle aggregation. For the organic/organic DN system, several studies have investigated the internal fracture of the sacrificial polymer network by using methodologies, such as mechanochromic cross-linkers[24] and mechanoradicals, which are generated by the fracture of a polymer chain[25]. These reports demonstrated that the fracture of the polymer chain occurred in the organic/organic DN via deformation. However, to the best of our knowledge, there has been no direct evaluation of the internal fracture of the sacrificial gel network using X-ray scattering.

In the organic/organic DN system, individual analysis of each polymer network is quite difficult because both networks are composed of organic polymers. However, in inorganic/organic DN systems, the internal fracture of the sacrificial network can be evaluated. The sacrificial networks in inorganic/organic DN ion gels are composed of a silica particle-based network. Because of the high electron density of silica particles, the network structure of a silica particle-based network can be directly analyzed by X-ray scattering. In this study, we directly evaluated the internal fracture of the silica particle network in the inorganic/organic DN ion gels using small angle X-ray scattering (SAXS). This is the first report to directly evaluate the internal fracture of the sacrificial gel network in inorganic/organic DN ion gels. The findings of this study could be used to improve the toughness of inorganic/organic DN ion gels.

Experimental Section

Materials

As an ionic liquid, 1-butyl-3-methylimidazolium bis(trifluoromethylsulfonyl)imide ([C_4mim][Tf_2N], Fig. S1(a)) (Sigma-Aldrich Co., St. Louis, MO , U.S.A.), was used after eliminating the dissolved water by bubbling dry nitrogen through the solution for more than 15 min. *N*,*N*-dimethylacrylamide (DMAAm, Tokyo Chemical Industry Co., Tokyo, Japan) as a monomer of PDMAAm (Fig. S1(b)), 2-oxoglutaric acid (OA, Tokyo Chemical Industry Co.) as a photo-radical initiator, and *N*,*N*'-methylenebis(acrylamide) (MBAA, Wako Pure Chemicals Industry Ltd., Osaka, Japan) as a chemical cross-linker of PDMAAm were used to form the organic PDMAAm network in the ionic liquid. DMAAm and OA were used as received. MBAA was used after purification by recrystallization in ethanol. Tetraethyl orthosilicate (TEOS, Sigma-Aldrich Co.) was used to form the silica particle network without further purification. Formic acid (Wako Pure Chemicals Industry Ltd.) was used as the solvolytic agent for the sol–gel reaction of TEOS without further purification. In the synthesis of linear PDMAAm for the adsorption test, 2,2'-azobis(isobutyronitrile) (AIBN, Wako Pure Chemicals Industry Ltd.) was used as the thermal-radical initiator after purification by recrystallization in ethanol.

Preparation of Inorganic/Organic DN Ion Gels and a PDMAAm Single Network (SN) Ion Gel

Inorganic/organic DN ion gels were prepared via a one-pot/two-step process by inducing a thermally initiated sol–gel reaction of TEOS and photic initiated free-radical polymerization of DMAAm in the ionic liquid.[15] For example, a precursor solution was prepared by mixing 7.92 g of [C_4mim][Tf_2N], 1.10 g of TEOS, 1.57 g of DMAAm (molar ratio of TEOS/DMAAm = 1/3 mol/mol), 9.8 mg of MBAA (0.4 % of DMAAm in mole), and 2.3 mg of OA (0.1 % of DMAAm in mole) until the solution became completely transparent. A total of 1.90 g of formic acid was added to the precursor solution and stirred until it was completely dissolved. The solution was injected in a mold consisting of two glass plates with a fluorinated ethylene propylene (FEP) copolymer film and a poly(tetrafluoroethylene) (PTFE) spacer (1.0 mm thickness), and placed in a thermostat oven at 323 K for 48 h for the silica particle network to form. Then, the ion gel was irradiated by 365 nm UV light for 9 h to achieve PDMAAm network formation. The obtained ion gel was maintained at 373 K for 12 h under a vacuum to remove the formic acid, unreacted monomer, and generated ethanol through the sol–gel reaction of TEOS. The compositions of the ionic liquid and the inorganic/organic network in the obtained ion gels were determined as 80.9 ± 0.1 and 19.1 ± 0.1 wt% (3.1 wt% of silica particle and 16 wt% of PDMAAm), respectively. The weights of the inorganic/organic skeleton were obtained via IL extraction using sufficient ethanol followed by drying in a vacuum at an elevated temperature. The silica particle and PDMAAm contents in the inorganic/organic skeleton were calculated from the weight ratio of a silica particle and PDMAAm, which were obtained by thermogravimetric (TG) measurement. The weight of IL was obtained by subtracting the weight of the inorganic/organic skeleton from the weight of the ion gel. A PDMAAm single-network (SN) ion gel was also prepared in the same manner without using the chemicals for the sol–gel reaction of TEOS. The content of [C_4mim][Tf_2N] in the PDMAAm SN ion gel was adjusted to 84 wt % to keep the composition of PDMAAm the same in both the SN ion gel and inorganic/organic DN ion gels (*ca*. 16 wt %). To evaluate the effect of silica particle content on the dissipated energy of the inorganic/organic DN ion gels, we controlled the silica particle content from 1.7 wt% to 5.1 wt% with constant PDMAAm content, *ca.* 16 wt%.

Mechanical Property Measurement

A uniaxial stretch test of inorganic/organic DN ion gels was carried out using an automatic recording universal testing instrument (EZ-LX, Shimadzu Co., Kyoto, Japan) at 298 K. A dumbbell-shaped specimen (length, width, thickness: 75.0, 4.0, 1.0 mm) was used for the uniaxial stretching test. Because the inorganic/organic DN ion gels had no volatile components, the mechanical properties could be measured in an open environment without considering any composition change during the measurement. For all measurements, the sample was attached to the instrument at a distance of 35 mm between the jigs. A uniaxial stretching test was conducted by stretching the sample at a constant strain rate of 100 mm/min. In the cyclic loading–unloading test, the stretching and return operations were performed at the same strain rate of 100 mm/min. The dissipated energy U (kJ/m^3) was calculated from the cyclic loading-unloading curve using the following equation:

$$U = \int_1^{2.5} \sigma \, \mathrm{d}\lambda \Big|_{\text{loading}} - \int_1^{2.5} \sigma \, \mathrm{d}\lambda \Big|_{\text{unloading}} \quad (1)$$

where σ (kPa) is the stress, and λ (-) is the stretch ratio. In this study, the dissipated energy of the inorganic/organic DN ion gels is defined as the dissipated energy from λ = 1.0 to λ = 2.5.

Small Angle X-ray Scattering (SAXS) Measurement

SAXS experiments were performed at the RIKEN beamline BL45XU in a SPring-8 synchrotron radiation facility (Hyogo, Japan). The X-ray wavelength, distance between samples and the detector, and detector used were 0.155 nm, 3515 mm, and PILATUS 3X 2M (Dectris Ltd., Baden-Daettwil, Switzerland), respectively. The absorption and background scattering of the obtained two-dimensional data were corrected. The scattering vector q ($q = 4\pi\sin\theta/\lambda_{\text{X-ray}}$; θ is the scattering angle and $\lambda_{\text{X-ray}}$ is the wavelength of an incident X-ray beam (0.155 nm), respectively) and position of the incident X-ray beam on the detector were calibrated using several orders of layer reflections from silver behenate (d = 5.8380 nm). A dumbbell-shaped ion gel specimen (length, width, thickness: 75.0, 4.0, and 1.0 mm) of the inorganic/organic DN ion gels was used for the SAXS measurement. The specimen was attached to a uniaxial tensile tester in the SAXS setup. The specimen was stretched in a horizontal direction at a constant strain rate of 60 mm/min from its original state by a stretch ratio λ = 2.5 and returned to the original state. The SAXS patterns were continuously captured with an exposure time of 1 s from λ = 1.0 to λ = 2.5 in the loading and unloading process. For all the cases of SAXS analysis, the scattering profiles from PDMAAm SN ion gel at each stretch ratio were subtracted from the original SAXS pattern to evaluate the scattering from the silica particle network. The q-profiles in the tensile direction were scanned from the horizontal area with an azimuthal angle range of ±15°.

Fourier-Transform Infrared (FT-IR) Spectroscopy Measurement

FT-IR spectra (Nicolet iS5vFT-IR, Thermo Scientific Inc., Waltham, U.S.A) of the ILs and DN ion gels were measured to confirm the H-bond formation between PDMAAm and the surface of silica particle. Small cut inorganic/organic DN ion gels were used for the FT-IR measurement. The attenuated total reflection (ATR) method was used for the FT-IR measurements.

Adsorption Test

[C_4mim][Tf_2N] and PDMAAm can adsorb onto the surface of a silica particle. If [C_4mim][Tf_2N] or PDMAAm preferentially adsorb onto the silica particle, the adsorption behavior can be detected by the composition change of [C_4mim][Tf_2N]/PDMAAm along with the adsorption of [C_4mim][Tf_2N] or PDMAAm onto the surface of a silica particle via the adsorption test. In this test, the linear PDMAAm, which was synthesized by free-radical polymerization, was used. A total of 7.0 g of DMAAm, 0.12 g of AIBN (1.0 % of DMAAm in mole) was mixed with super dehydrated 1,4-dioxane in a nitrogen substituted three-neck round-bottom flask. After bubbling dry nitrogen in 1,4-dioxane for more than 30 min, free-radical polymerization was performed at 343 K for 24 h. The linear PDMAAm solution was precipitated into diethyl ether. The obtained linear PDMAAm was maintained at 373 K for 12 h under a vacuum to remove the residual organic solvent. For the adsorption rest, the PDMAAm/[C_4mim][Tf_2N] solution was prepared using a cosolvent method. Linear PDMAAm was dissolved in ethanol. Then, IL was added to the solution. The solution was evaporated at 373 K for 12 h under a vacuum to remove the cosolvent ethanol. The PDMAAm concentration in the IL solution was adjusted to about 1 wt%. For the adsorption test, various amounts of silica particles with a diameter of 75 μm (Silica Gel 60, spherical neutrality, NACALAI TESQUE, INC., Kyoto, Japan) were added to the 1.0 g of PDMAAm/[C_4mim][Tf_2N] solution. The mixture was stirred at 298 K for 6 h. The supernatant was removed by decantation; then, the [C_4mim][Tf_2N]/DMAAm unit ratio was measured by ^{1}H NMR (JCZ-400, JEOL RESONANCE Inc., Tokyo, Japan). In this experiment, μm-sized silica particles were used to completely precipitate the silica particles. It was confirmed that the adsorption equilibrium could be reached in less than 6 h. The [C_4mim][Tf_2N]/DMAAm unit ratio was calculated from the integral ratio of N-(CH_3)$_2$ in PDMAAm and CH_3 in [C_4mim][Tf_2N] as determined by the ^{1}H NMR measurement.

SiO_2/PDMAAm Ratio Measurement

Thermogravimetric (TG) measurement of the inorganic/organic composite skeleton was performed to calculate the SiO_2/PDMAAm ratio. The inorganic/organic composite skeleton was obtained from the inorganic/organic DN ion gels via IL extraction using a sufficient amount of ethanol followed by drying in a vacuum at an elevated temperature. The TG measurement were conducted using open Pt pans on a thermogravimetry-differential thermal analysis device (TG-DTA Thermo plus EVOII, Rigaku Co., Tokyo, Japan) from 373 K to 1273 K at a heating rate of 10 K/min under a pure air (TAIYO NIPPON SANSO CORPORATION, Tokyo, Japan) atmosphere. Before the measurement, the sample atmosphere was maintained at 373 K for 2 h to remove the absorbed water. The

PDMAAm weight fraction was calculated by the weight loss from 373 K to 1273 K. The SiO_2 weight fraction was calculated by the residual weight at 1273 K.

Results and Discussion

Interaction between PDMAAm and Silica Particles

In general, PDMAAm strongly adsorbs onto silica particles in aqueous media.[26–28] For the silica particle/PDMAAm composite network in a hydrogel, it was reported that the silica particle/PDMAAm composite hydrogel showed mechanical hysteresis via the desorption/readsorption of PDMAAm onto the silica particles.[27] Based on this report, the desorption/readsorption of PDMAAm on silica particles may contribute to energy dissipation even in ion gels. Thus, it is worth investigating the adsorption of PDMAAm onto silica particles in inorganic/organic DN ion gels. The interaction between PDMAAm and silica particles was evaluated by FT-IR spectra. Fig. 1 shows the FT-IR spectra of the inorganic/organic DN ion gels with various silica particle contents. The FT-IR spectra of inorganic/organic DN ion gels showed an absorbance peak at 1633 cm^{-1}, which was attributed to the stretch vibration of the C=O group in PDMAAm. As shown in Fig. 1, the absorbance wavenumber of the stretch vibration of the C=O group was constant with increasing silica particle content. If PDMAAm formed an H-bond with the Si-OH group on the surface of a silica particle, the absorbance peak of the stretch vibration of the C=O group would shift to a lower wavenumber.[29] Thus, the FT-IR results shown in Fig. 1 demonstrated that PDMAAm did not form an H-bond with the Si-OH group on the surface of the silica particle. In the aqueous system, the strong interaction between PDMAAm and the silica particle was attributed to the formation of an H-bond between the C=O group in PDMAAm and the Si-OH group on the surface of the silica particle.[26] It was speculated that PDMAAm did not adsorb onto the surface of the silica particle because of the negligibly low interaction between PDMAAm and the silica particles in the ion gels.

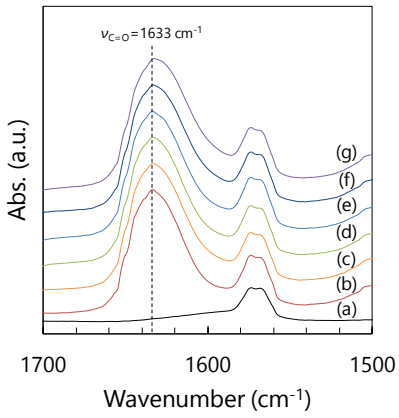

Fig. 1 FT-IR spectra of inorganic/organic DN ion gels with various silica particle content. Pure IL(a), SiO_2/PDMAAm (weight ratio) = 0 (b), 0.11 (c), 0.13 (d), 0.17 (e), 0.20 (f), and 0.29 (g).

The ability of PDMAAm to adsorb onto a silica particle was evaluated by an adsorption test in IL medium. In this experiment, the μm-sized silica particle (diameter is 75 μm) was used to achieve complete precipitation of the silica particle in IL. The primary diameter of the silica particle formed in the inorganic/organic DN ion gel was 6–10 nm.[16] Therefore, the adsorption amount of PDMAAm or [C_4mim][Tf_2N] on the silica particle in the adsorption test was different in the inorganic/organic DN ion gel. However, a qualitative evaluation was possible because both types of silica particles in the adsorption test and inorganic/organic DN ion gels had similar surface conditions, i.e., both surfaces were composed of Si-OH groups. The relationship between [C_4mim][Tf_2N]/DMAAm unit ratio and added silica particle amount was shown in Fig. 2. The [C_4mim][Tf_2N]/DMAAm unit ratio in the supernatant monotonically decreased with silica particle content. This result demonstrated that IL molecules preferentially adsorbed onto the silica particle in the IL medium. Thus, it was concluded that the ability of PDMAAm to adsorb onto the silica particle was quite lower than that of the IL molecule. In other words, it was indicated that the PDMAAm hardly interacted with silica particles and did not adsorb onto the silica particle. In general, the IL molecules can adsorb onto the silica particle via attractive interactions such as electrostatic interactions and H-bonds.[30] Based on these results, it was suggested that PDMAAm could not adsorb onto the silica particle, as IL molecules have higher adsorption ability than PDMAAm in competitive adsorption. It was concluded that the desorption/readsorption of PDMAAm onto the surface of a silica particle hardly contributed to the energy dissipation of inorganic/organic DN ion gels.

Internal Fracture of Silica Particle Network

To evaluate the internal fracture of the silica particle network in the inorganic/organic DN ion gels clearly, the SAXS measurement was performed for inorganic/organic DN ion gels during a uniaxial loading–unloading deformation process. The scattering intensity $I(q)$ of fractal-like aggregates of primary particles is given by Eq. (2).

$$I(q) = A \cdot F(q) \cdot S(q) + I_{TDS}(q) \quad (2)$$

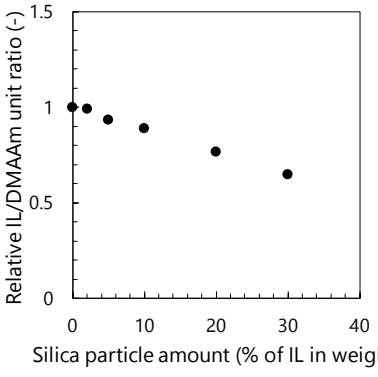

Fig. 2 Relationship between the relative [C_4mim][Tf_2N]/DMAAm unit ratio in the supernatant and added silica particle amount.

where A is a constant, $F(q)$ the form factor of an individual scatter, $S(q)$ is an effective structure factor, and $I_{TDS}(q)$ is thermal diffuse scattering (TDS). For a spherical system, the form factor $F(q)$ is expressed as the following function:

$$F(q) = \int_0^\infty \left[3\left\{\frac{\sin(qr) - qr\cos(qr)}{(qr)^3}\right\}\right]^2 \rho(r)\,\mathrm{d}r \quad (3)$$

where r and $\rho(r)$ are the particle radius and its probability density, respectively. It is assumed that the particle radii are normally distributed around an averaged radius of 3 nm, which was determined from the TEM image shown in Fig. S2. An approach for $S(q)$ accounting for the cutoff ξ at low-q can be cast as the following function[31,32]:

$$S(q) = 1 + \frac{C \cdot \Gamma(D-1) \cdot \xi^D \cdot \sin((D-1) \cdot \arctan(q\xi))}{(1+q^2\xi^2)^{(D-1)/2} \cdot q\xi} \quad (4)$$

where C is a constant, D is the fractal dimensionality, and $\Gamma(D\text{-}1)$ is the gamma function of argument D-1. ξ represents the characteristic distance above which the mass distribution is no longer described by the fractal law. In practice, ξ is assimilated to the size or correlation length of an aggregate, and it can be interchanged with the classical radius of gyration R_g, deduced from Guinier's law, as the two sizes, ξ and R_g, are linked by a linear function depending on D. [32,33] $I_{TDS}(q)$ is approximated by the following equation[34,35]:

$$I_{TDS}(q) = I_{TDS}(0) \cdot \exp(cq^2) \quad (5)$$

where c is a constant, and $I_{TDS}(0)$ is an extrapolated scattering intensity at q = 0. The structural change of the silica particle network during the uniaxial loading–unloading deformation was estimated by the ξ value, i.e., the aggregation size of the silica particle network.

The 1D-SAXS Kratky profiles ($q^2 \cdot I(q)$ vs. q plot) in the tensile direction of the inorganic/organic DN ion gel under various stretch ratios are shown in Fig. 3. The original $I(q)$ vs. q plots are shown in Fig. S3. Because the clear difference of SAXS profiles could not be observed in the original plot as shown in Fig. S3, we chose Kratky plot to clearly show the difference of each SAXS profile. In this measurement, the SAXS profile of λ = 1.0 could not be obtained under unloading processing conditions because the sample position was shifted from beam position owing to the deflection by the residual strain of the inorganic/organic DN ion gel. All of the SAXS profiles shown in Fig. 3 were attributed to the silica particle network because the scattering from the PDMAAm SN ion gel, which is composed of only a PDMAAm network and IL at each stretch ratio, were subtracted from the original SAXS pattern. The background analysis is based on an assumption that the SAXS profile of the PDMAAm is not influenced by the introduction of the silica particles. According to the report by Inoue et al., the deformation behavior of polymer in rubber was affected by the silica particles.[36] In the case of rubber system, strong interaction was formed between polymer and filler particles. However, in contrast to the case of rubber system, we demonstrated that the interaction between PDMAAm and silica particle in the inorganic/organic DN ion gels was negligibly low (Figs. 1 and 2). In addition, the scattering intensity from silica particle was much higher than that from PDMAAm network because of the high electron density of silica particle. The SAXS profiles of inorganic/organic DN ion gel and PDMAAm SN ion gel without background analysis are shown in Fig. S4. The scattering intensity of inorganic/organic DN ion gel was about 100 times higher than that of PDMAAm ion gel. Based on this result, even if the deformation behavior of PDMAAm network was affected by the silica particle, it was considered that the effect on the SAXS profile was negligibly low. As shown in Fig. 3, the SAXS profiles drastically changed with the uniaxial loading–unloading deformation process, especially in the low-q region. In addition, it should be noted that the SAXS profiles obtained from the unloading process were not consistent with those of the loading process. This result demonstrated that the network structure of the silica particle network irreversibly changed with uniaxial stretch deformation.

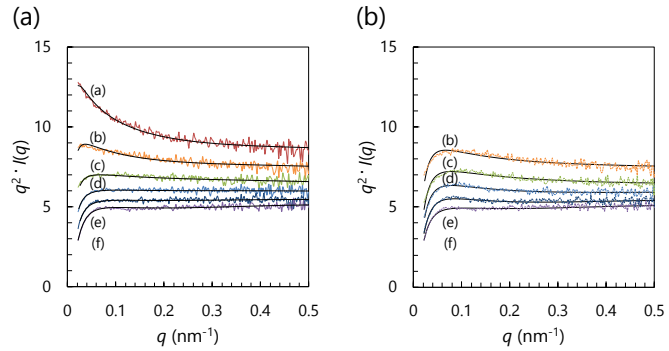

Fig. 3 1D-SAXS Kratky profiles ($q^2 \cdot I(q)$ vs. q plot) in the tensile direction of the inorganic/organic DN ion gel at various stretch ratios: (a) loading process and (b) unloading process. The black solid lines in Fig. 3(a) and Fig. 3(b) represents the fitting of curves obtained with Eqs. (2)–(5). λ = 1.0 (a), 1.3 (b), 1.6 (c), 1.9 (d), 2.2 (e), and 2.5 (f).

Table 1 Values of the correlation length ξ, constants C and A, and fractal dimension D obtained from SAXS analysis of the inorganic/organic DN ion gel.

	Stretch ratio	ξ (nm)	C	D	A
Loading	1	129	0.29	2.16	28.05
	1.3	110	0.34	2.09	21.79
	1.6	91	0.38	2.04	13.33
	1.9	71	0.34	2.04	17.80
	2.2	56	0.30	2.07	17.22
	2.5	45	0.30	2.09	14.35
Unloading	2.2	42	0.27	2.15	16.34
	1.9	44	0.26	2.15	20.41
	1.6	47	0.30	2.15	20.59
	1.3	54	0.30	2.11	24.94

To evaluate the structural change of the silica particle network quantitatively, the SAXS profiles were analyzed using Eqs. (2)–(5). As shown in Fig. 3, all scattering intensity profiles can be sufficiently described by Eqs. (2)–(5). The obtained fitting parameters, ξ, D, C, and A, are summarized in Table 1. The parameter A depended on the total volume of the primary particles.[37] In other words, the parameter A depends on the

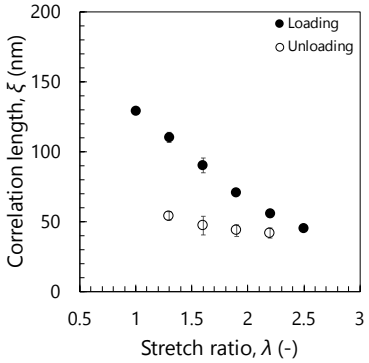

Fig. 4 Relationship between the correlation length of the silica particle network in the inorganic/organic DN ion gel and stretch ratio.

thickness of the ion gel. Thus, it can be considered that the parameter *A* decreased during the uniaxial loading process because the ion gel thickness decreased with uniaxial stretching. On the other hand, during the unloading process, the ion gel thickness increased, and the parameter *A* also increased. The stretch ratio dependency of the correlation length of an aggregate, ξ, is shown in Fig. 4. The correlation length of the silica particle network monotonically decreased with increasing stretch ratio. In addition, the correlation length that decreased during the loading process was not recovered in the unloading process (Table 1).

If the silica particle network were not fractured by uniaxial stretch, the change in the correlation length would show the same trend as the macroscopic sample deformation, i.e., the correlation length should increase with increasing stretch ratio in the tensile direction. For example, in a silica aerogel system, the correlation length decreased for the compression axis and increased for the perpendicular axis with uniaxial compression.[38] In the silica aerogel system, the trends of correlation length and macro sample deformation were consistent. In the inorganic/organic DN ion gels, the trend of correlation length dependency on macro sample deformation was opposite to that observed in the silica aerogel system because the correlation decreased while the macro sample length increased. This result indicated that the fractal aggregation structure of the silica particle network was fractured by uniaxial stretch deformation. Based on these results, the internal fracture of sacrificial network successfully demonstrated by using the inorganic/organic DN system. These results confirmed that the internal fracture of sacrificial network which is suggested in the organic/organic DN systems also occurred in the inorganic/organic DN system. It should be noted that the correlation between strain and the decrease in aggregation size of the particles does not necessarily mean that the disaggregation is the primary energy-dissipation mechanism. We should consider that there could be stronger interactions that are breaking simultaneously. However, as mentioned before, the interaction between PDMAAm and silica particle in the inorganic/organic DN ion gels was negligibly low. Therefore, we considered that the energy dissipation of the inorganic/organic DN ion gels were mainly attributed to the internal fracture of the silica particle network.

Table 2 [C_4mim][Tf_2N] content, silica particle content, and PDMAAm content of the DN ion gel prepared with various DMAAm/TEOS molar ratios.

SiO_2/PDMAAm	IL content (wt%)	Silica particle content (wt%)	PDMAAm content (wt%)
0.29	77.5	5.1	17.4
0.20	80.9	3.1	16.0
0.17	81.4	2.7	15.9
0.13	82.1	2.0	15.9
0.11	82.6	1.7	15.7

Relationship between Silica Particle Content and Dissipated Energy

The dissipated energy of the inorganic/organic DN ion gels should depend on the silica particle content because the energy dissipation of an inorganic/organic DN ion gel is caused by the internal fracture of the silica particle network. The energy dissipation in the inorganic/organic DN ion gels were attributed to the fracture of inter-silica particle interactions such as van der Waals attraction and hydrogen bonding in the IL medium.[15,16] Thus, the total surface area of the silica particles would strongly affect the dissipated energy of the inorganic/organic DN ion gels. Based on this hypothesis, the effect of the silica particle content of the inorganic/organic DN ion gels on the energy dissipation was evaluated under constant PDMAAm content condition. Table 2 shows the [C_4mim][Tf_2N]/silica particle/PDMAAm composition of the inorganic/organic DN ion gels used in this experiment. All of the inorganic/organic DN ion gels contained a constant amount of PDMAAm, *ca*. 16 wt%. On the other hand, the silica particle content in the inorganic/organic DN ion gels could be successfully controlled from 1.7 wt% to 5.1 wt%. Fig. 5 shows the stress–stretch curves of the inorganic/organic DN ion gels with various silica particle contents. The stress–stretch curves clearly demonstrated that the fracture stress and toughness of

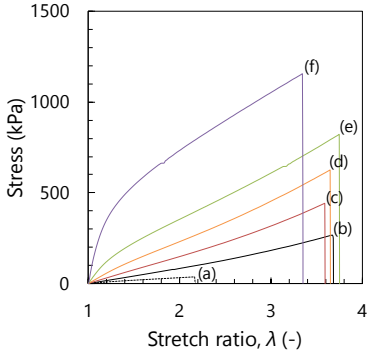

Fig. 5 Stress–stretch curves of the inorganic/organic DN ion gels with various silica particle content. SiO_2/PDMAAm (weight ratio) = 0 (a), 0.11 (b), 0.13 (c), 0.17 (d), 0.20 (e), and 0.29 (f).

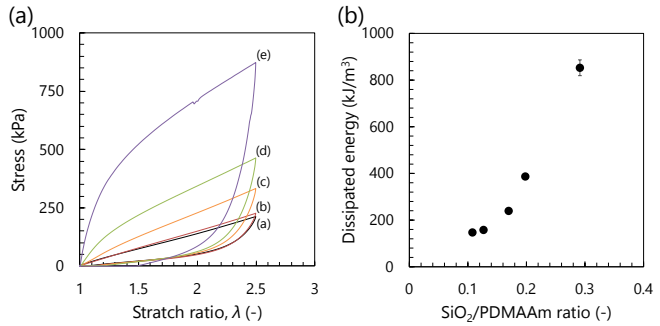

Fig. 6 (a) Cyclic loading–unloading curves of the inorganic/organic DN ion gels and (b) relationship between dissipated energy and silica particle content. SiO_2/PDMAAm (weight ratio) = 0.11 (a), 0.13 (b), 0.17 (c), 0.20 (d), and 0.29 (e).

the inorganic/organic DN ion gels increased with increasing silica particle content. On the other hand, the fracture stretch ratio (stretch ratio at fracture point) was independent of SiO_2/PDMAAm ratio except for the case of SiO_2/PDMAAm = 0 (PDMAAm SN ion gel) in the range of 3.4–3.8. This is because the fracture stretch ratio was dominated by the PDMAAm network, which was prepared with the same cross-linker concentration (0.4 % of DMAAm in mole) for all of theinorganic/organic DN ion gels.

To investigate the effect of silica particle content on the fracture stress of the inorganic/organic DN ion gels in detail, the dissipated energy was calculated from the cyclic loading–unloading curves shown in Fig. 6(a) using Eq. (1). In general, the viscoelastic material shows the hysteresis without any structural changes. However, we consider that the viscoelastic effect was negligibly small in the stress–strain curve for the viscoelastic ion gels measured under our experimental condition. The experimental evidence is found in the cyclic loading–unloading curves of PDMAAm SN ion gel shown in Fig. S5. As clearly shown in Fig. S5, the stress–strain curves of PDMAAm SN ion gel did not show any hysteresis although PDMAAm SN ion gel was also viscoelastic material. In addition, we reported the inorganic/organic composite ion gel with well dispersed silica particles did not show mechanical hysteresis.[15] Based on these results, we consider that the viscoelastic effect in stress–strain curves is negligibly small. As shown in Fig. 6(b), the dissipated energy drastically increased with increasing silica particle content in the inorganic/organic DN ion gels. This result indicated that the dissipated energy of the inorganic/organic DN ion gel was dominated by the total surface area of the silica particle. Thus, the fracture stress and toughness of the inorganic/organic DN ion gels increased with increasing dissipated energy owing to an increase in silica particle content.

Summary and Conclusion

The energy dissipation in inorganic/organic DN ion gels has been considered to be due to the internal fracture of a sacrificial silica particle network, which is preferentially fractured by deformation. However, to the best of the authors' knowledge, no publications are available in the literature that discuss the internal network fracture of the silica particle network based on direct approaches. In this report, we directly evaluated the internal fracture phenomenon of the silica particle network in inorganic/organic DN ion gels using SAXS analysis. The SAXS analysis clearly demonstrated that the aggregation size of the silica particle network irreversibly decreased with uniaxial stretch. FT-IR spectra and an adsorption test indicated that the PDMAAm hardly interacted with the silica particles and did not adsorb to the silica particles. The dissipated energy of the inorganic/organic DN ion gels increased with increasing silica particle content. Based on these results, we concluded that the energy dissipation of the DN ion gels can be attributed to the internal fracture of the silica particle network. The internal fracture behavior could be described as the irreversible decrease of aggregation size of silica particle network. This report directly demonstrates that the energy dissipation mechanism of inorganic/organic DN ion gels is caused by the internal fracture of the gels' silica particle network.

Conflicts of interest

There are no conflicts to declare.

Acknowledgements

The synchrotron radiation experiments were performed using the SPring-8 BL45XU with the approval of the Japan Synchrotron Radiation Research Institute (JASRI) (Proposal No. 2018A1659 and 2018B1690). The authors thank the Research Facility Center for Science and Technology of Kobe University for providing the FE-TEM for use in this study. Parts of this work were supported by KAKENHI (18K04812 and 19J11528) of the Japan Society for the Promotion of Science (JSPS).

Notes and references

1 A. Noda and M. Watanabe, *Electrochim. Acta*, 2000, **45**, 1265–1270.
2 T. Ueki and M. Watanabe, *Macromolecules*, 2008, **41**, 3739–3749.
3 T. P. Lodge, *Science*, 2008, **321**, 50–51.
4 J. E. Bara, E. S. Hatakeyama, D. L. Gin and R. D. Noble, *Polym. Adv. Technol.*, 2008, **19**, 1415–1420.
5 S. Kasahara, E. Kamio, A. Yoshizumi and H. Matsuyama, *Chem. Commun.*, 2014, **50**, 2996–2999.
6 F. Moghadam, E. Kamio, A. Yoshizumi and H. Matsuyama, *Chem. Commun.*, 2015, **51**, 13658–13661.
7 F. Ranjbaran, E. Kamio and H. Matsuyama, *J. Membr. Sci.*, 2017, **544**, 252–260.
8 S. Kasahara, E. Kamio, R. Minami and H. Matsuyama, *J. Membr. Sci.*, 2013, **431**, 121–130.
9 K. Fujii, H. Asai, T. Ueki, T. Sakai, S. Imaizumi, U. Chung, M. Watanabe and M. Shibayama, *Soft Matter*, 2012, **8**, 1756–1759.
10 Y. Gu, S. Zhang, L. Martinetti, K. H. Lee, L. D. Mcintosh, C. D. Frisbie and T. P. Lodge, *J. Am. Chem. Soc.*, 2013, **135**, 9652–9655.
11 F. Moghadam, E. Kamio and H. Matsuyama, *J. Membr. Sci.*, 2017, **525**, 290–297.
12 Y. Ding, J. Zhang, L. Chang, X. Zhang, H. Liu and L. Jiang, *Adv. Mater.*, 2017, **29**, 1704253.
13 F. Moghadam, E. Kamio, T. Yoshioka and H. Matsuyama, *J. Membr. Sci.*, 2017, **530**, 166–175.

14 14 H. Arafune, S. Honma, T. Morinaga, T. Kamijo, M. Miura, H. Furukawa and T. Sato, *Adv. Mater. Interfaces*, 2017, 4, 1700074.
15 E. Kamio, T. Yasui, Y. Iida, J. P. Gong and H. Matsuyama, *Adv. Mater.*, 2017, **29**, 1704118.
16 T. Yasui, E. Kamio and H. Matsuyama, *Langmuir*, 2018, **34**, 10622–10633.
17 J. P. Gong, *Soft Matter*, 2010, **6**, 2583–2590.
18 J. Y. Sun, X. Zhao, W. R. K. Illeperuma, O. Chaudhuri, K. H. Oh, D. J. Mooney, J. J. Vlassak and Z. Suo, *Nature*, 2012, **489**, 133–136.
19 Q. Chen, L. Zhu, C. Zhao, Q. Wang and J. Zheng, *Adv. Mater.*, 2013, **25**, 4171–4176.
20 M. A. Haque, T. Kurokawa, G. Kamita and J. P. Gong, *Macromolecules*, 2011, **44**, 8916–8924.
21 T. Nakajima, Y. Fukuda, T. Kurokawa, T. Sakai, U. Il Chung and J. P. Gong, *ACS Macro Lett.*, 2013, **2**, 518–521.
22 J. Hu, K. Hiwatashi, T. Kurokawa, S. M. Liang, Z. L. Wu and J. P. Gong, *Macromolecules*, 2011, **44**, 7775–7781.
23 T. Hashimoto, N. Amino, S. Nishitsuji and M. Takenaka, *Polym. J.*, 2019, **51**, 109–130.
24 E. Ducrot, Y. Chen, M. Bulters, R. P. Sijbesma and C. Creton, *Science*, 2014, **344**, 186–189.
25 T. Matsuda, R. Kawakami, R. Namba, T. Nakajima and J. P. Gong, *Science*, 2019, **363**, 504–508.
26 D. Hourdet and L. Petit, *Macromol. Symp.*, 2010, **291–292**, 144–158.
27 W. C. Lin, W. Fan, A. Marcellan, D. Hourdet and C. Creton, *Macromolecules*, 2010, **43**, 2554–2563.
28 S. Rose, A. Prevoteau, P. Elzière, D. Hourdet, A. Marcellan and L. Leibler, *Nature*, 2013, **505**, 382–385.
29 R. Tamaki, K. Naka and Y. Chujo, *Polym. J.*, 1998, 30, 60–65.
30 Z. He and P. Alexandridis, *Phys. Chem. Chem. Phys.*, 2015, **17**, 18238–18261.
31 T. Freltoft, J. K. Kjems and S. K. Sinha, *Phys. Rev. B*, 1986, **33**, 269–275.
32 J. Teixeira, *J. Appl. Crystallogr.*, 1988, **21**, 781.
33 S. Coste, A. Lecomte, P. Thomas and J. C. Champarnaud-Mesjard, *Langmuir*, 2008, **24**, 12568–12574.
34 J. Rathje and W. Ruland, *Colloid Polym. Sci.*, 1976, **254**, 358–370.
35 T. Koga, T. Hashimoto, M. Takenaka, K. Aizawa, N. Amino, M. Nakamura, D. Yamaguchi and S. Koizumi, *Macromolecules*, 2008, **41**, 453–464.
36 T. Inoue, Y. Narihisa, T. Katashima, S. Kawasaki and T. Tada, *Macromolecules*, 2017, **50**, 8072–8082.
37 V. Torma, H. Peterlik, U. Bauer, W. Rupp, N. Hüsing, S. Bernstorff, M. Steinhart, G. Goerigk and U. Schubert, *Chem. Mater.*, 2005, **17**, 3146–3153.
38 J. Pollanen, K. R. Shirer, S. Blinstein, J. P. Davis, H. Choi, T. M. Lippman, W. P. Halperin and L. B. Lurio, *J. Non. Cryst. Solids*, 2008, **354**, 4668–4674.

